# Electronic Supplementary Material

**One stone, three birds: up-conversion, photothermal and p-n heterojunction to boost BiOBr:$Yb^{3+}$,$Er^{3+}$/$Cu_3Mo_2O_9$ full spectrum photodegradation**

Xintong Yao[1], Dong Zhang[2], Yupeng Liu[1], Yanzhao Chen[1], Dafeng Zhang (✉)[1], Junchang Liu[1], Xue-Yang Ji[1], Hengshuai Li[2], Peiqing Cai[3], Xipeng Pu (✉)[1]

1 School of Materials Science and Engineering, Shandong Provincial Key Laboratory of Chemical Energy Storage and Novel Cell Technology, Liaocheng University, Liaocheng 252000, China

2 School of Physics Science and Information Technology, Shandong Key Laboratory of Optical Communication Science and Technology, Liaocheng University, Liaocheng 252000, China

3 College of Optical and Electronic Technology, China Jiliang University, Hangzhou 310018, China

E-mails: dafengzh@hotmail.com (Zhang D), xipengpu@hotmail.com (Pu X)

## 1. Sample preparation

### 1.1 Materials

Bismuth nitrate pentahydrate ($Bi(NO_3)_3·5H_2O$), urea, yttrium oxide ($Yb_2O_3$), erbium oxide ($Er_2O_3$), ammonium bromide ($NH_4Br$), ethylenediaminetetraacetic acid disodium salt (EDTA-2Na), L-Histidine (L-HIS), isopropyl alcohol (IPA), polyvinylpyrrolidone (PVP) and ethylene glycol (EG) were purchased from Aladdin Co, Ltd., China. Concentrated nitric acid, anhydrous cupric sulfate ($CuSO_4$) and Sodium molybdate dihydrate were ($Na_2MoO_4·2H_2O$) were bought from Sinopharm Chemical Reagent Co., Ltd., China. All the chemicals are analytically pure and utilized without any additional purification.

### 1.2 Synthesis of BiOBr:$Yb^{3+}$,$Er^{3+}$(BYE)

The BYE was prepared by one-step combustion method. First, 4.062 g $Bi(NO_3)_3·5H_2O$ and 1.802 g urea were added in 25 mL mixed solution with 15 mL 0.1 M $Yb(NO_3)_3$ and 10 mL 0.02 M $Er(NO_3)_3$, and stirred for 15 min. Next, 2.928 g $NH_4Br$ was dissolved in above suspension liquid and stirred for 10 min, the suspension changes from white to pale yellow. Thereafter, the suspension-containing beaker was then move to a heating mantle at 350 ℃ to achieve gently evaporation until the solution is

sol-like. And then get heated till combustion reaction occurs, which is the exothermic redox reaction between urea and nitrates, the pale yellow BYE sample was prepared. BiOBr was synthesized by a similar way without the addition of $Yb(NO_3)_3$ and $Er(NO_3)_3$.

### 1.3 Synthesis of $Cu_3Mo_2O_9$ (CMO)

The CMO was synthesized by a simple hydrothermal method. Typical, the solution A was prepared by adding 0.749 g $CuSO_4$ in 30 mL deionized water and stirring for 20 min. The solution B was obtained by dissolving 0.726 g $Na_2MoO_4 \cdot 2H_2O$ and 0.16 g PVP in 30 mL deionized water. Then the solution A was added dropwise to the solution B and vigorous stirring 30 min to produce a pale-green suspension. Thereafter, the suspension was transferred into a 100 mL Teflon-lined autoclave and heated at 110 ℃ for 10 h to obtain a light green precursor. The precursor was washed and dried and placed in the crucible for calcination at 500 ℃ for 3 h in the air atmosphere.

### 1.4 Synthesis of BYE/CMO

The BYE/CMO composites were prepared by a simple ultrasonic assisted grinding calcination method. Briefly, 0.4 g BYE and a specified amount of CMO were mixed and ultrasonic with 20 mL ethanol for 30 min. and then the suspension was ground until dried in an agate mortar. Finally, the resultant composites were calcination at 160 ℃ for 2 h to form a tight coupling. The obtained samples were denoted as BYE/CMO-x (x = 3, 5, 10 and 15). Here, x indicates the mass ratio of CMO to BYE.

## 2. Characterization

X-ray diffractometer (XRD, D8 Advance, Bruker Co, Germany) was used to ensure the phase composition and crystallinity of samples. The X-ray source is Cu Kα-radiation (λ =1.5406 Å), and the scanning speed was 6 °/min. The morphologies of the samples were investigated by a Scanning electron microscopy (SEM, Zeiss Ltd., Germany) and a transmission electron microscopy (TEM, JEOL Ltd, Japan). The elemental composition and distribution of sample was performed with an energy-dispersive X-ray spectrometer (EDS) attachment on the SEM. A thermo ESCALAB 250Xi photoelectron spectrometer (XPS, Thermo Fisher Scientific, USA) with Al Kα-radiation was used to investigate the chemical stated of the samples. UV-3600 spectrophotometer (Shimadzu, Japan) was used to obtain the diffuse reflectance spectra (DRS) of samples and absorption spectra of MB solution.

A Hitachi F7000 fluorescence spectrophotometer was used to capture photoluminescence (PL) spectra of materials with an excited wavelength at 325 nm. Thermal images were taken with a thermal imager (TiS60+, Fluke Co., USA).

In order to evaluate the visible and NIR light photocatalytic performance of samples, methylene blue (MB) was used as pollutant models. The visible and NIR light sources are a 1000 W halogen lamp (Philips) with a JB420 cutoff filter ($\lambda > 420$ nm) and a 250 W infrared lamp (Philips) with an IR cutoff filter (JB 760, $\lambda > 760$ nm), respectively. In the photoreduction experiment, 50 mg of the photocatalyst was added into 100 mL of aqueous MB solution (10 mg/L). The suspension was stirred in dark for 30 min to achieve adsorption and desorption equilibrium. Then the concentration of MB solution was monitored by recording the absorption band maximum of 664 nm in the absorption spectra, respectively, and taken as the initial concentration ($C_0$). After the light was turned on, 3 mL of the suspension was extracted and centrifuged at regular intervals, whose MB concentration was analyzed by measured the absorption (C) of MB. To test the photostability of as synthesized samples, four-run cycling photocatalytic tests were carried out.

## 3. Photoelectrochemical measurements

All photoelectrochemical tests were performed on a 660D electrochemical workstation (Shanghai Chenhua Co., China) in a standard three-electrode system with a platinum wire and the saturated calomel electrode (SCE) as an auxiliary electrode and a reference electrode, respectively. The 0.1 M $Na_2SO_4$ aqueous solution was used as the electrolyte. The working electrode was prepared by dropping 30 μL suspension (10 mg photocatalyst was dissolved in a 0.5 mL mixed solution of isopropanol and water, and the volume ratio of 1:4) onto a 0.5 cm × 0.5 cm FTO glass, and then dried naturally at room temperature. The photocurrent responses, Nyquist plots and Mott-Schottky (MS) plots of samples were characterized in three-electrode system.

## 4. XAS Measurements

X-ray absorption spectrum (XAS) was recorded in fluorescence mode at the beamline 4B9A station of the Beijing Synchrotron Radiation Facility (BSRF). The measured data were processed with ATHENA, HAMA and ARTMIS IFEFFIT software packages to obtain X-ray absorption near-edge structure (XANES), Fourier transform extended X-ray absorption fine structure (FT-EXAFS) and

wavelet transform extended X-ray absorption fine structure (WT-EXAFS) spectra. Er and Yb $L_3$-edge $k^2$-weighted EXAFS spectra were obtained by normalizing with the edge-jump step, and $k^2$-weighted χ(k) data at the K edge were Fourier transformed to R space using hanning windows (dk = 1.0 $Å^{-1}$) to separate the EXAFS contributions.

## 5. Computational methods

First-principle calculations are based on density functional theory with CASTEP package of materials studio. The generalized gradient approximation (GGA) was used to deal with the electron-electron interactions, and the Perdew-Burke-Ernzerhof (PBE) function was used to deal with the exchange correlation. The thickness of the air layer was set to 15 Å to avoid the mutual influence between layers. The distance between BYE and CMO was set to 3 Å to form a BYE/CMO heterojunction. The work function can be calculated by the following formula: $\varphi=V(\infty)-E_F$, where $V(\infty)$ and $E_F$ are the electrostatic potential in a vacuum region far from the neutral surface and the Fermi energy of the neutral surface system, respectively.

## 6. Results and discussion

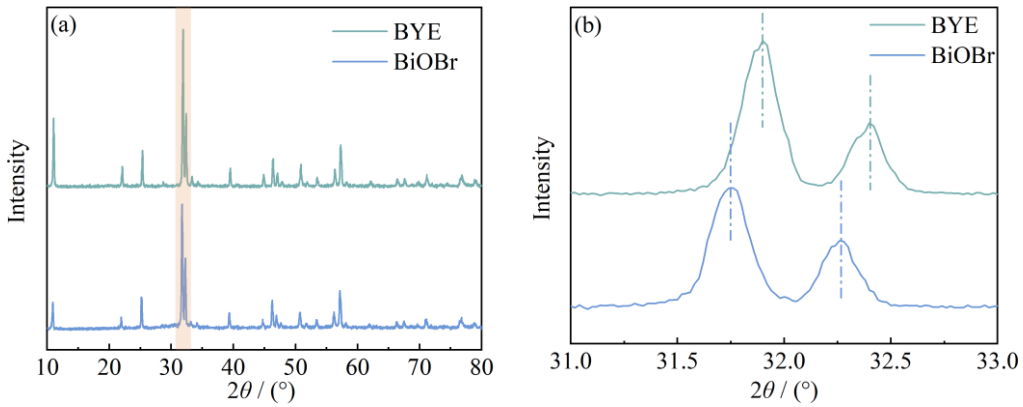


Fig. S1 (a) XRD patterns of BiOBr and BYE and (b) the main diffraction peaks from 31.0° to 33.0°

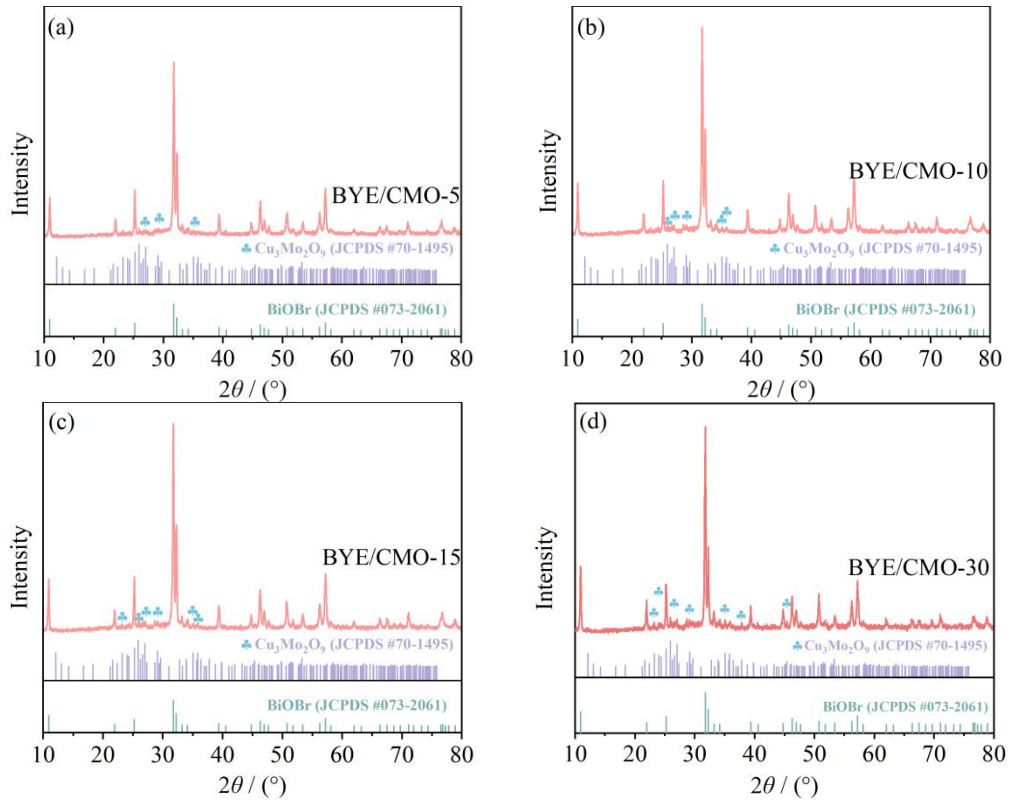


Fig. S2 The XRD patterns of (a) BYE/CMO-5, (b) BYE/CMO-10, (c) BYE/CMO-15 and (d) BYE/CMO-30 samples.

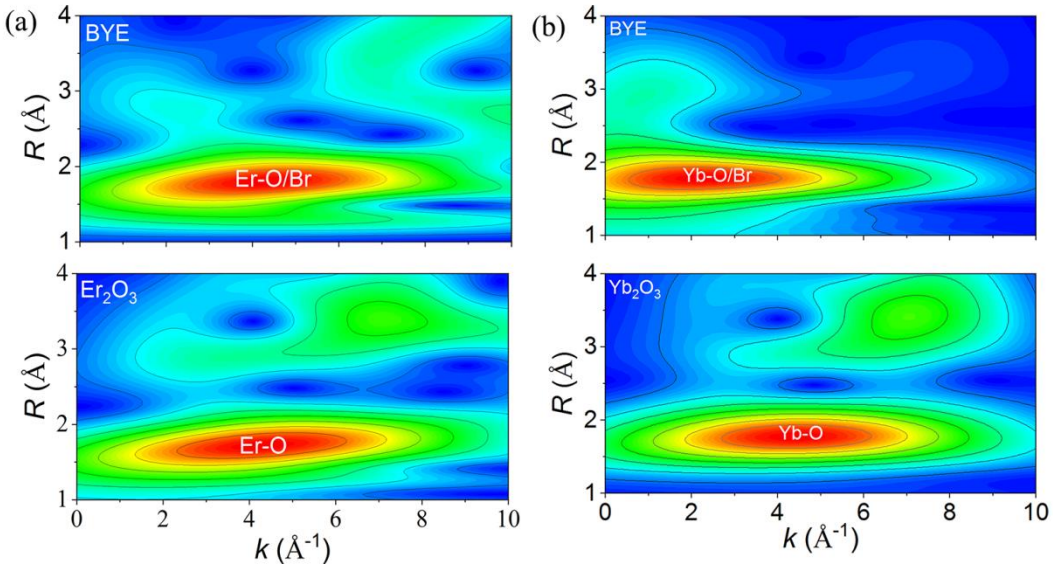


Fig. S3 WT-EXAFS spectra at the (a) Er $L_3$-edge and (b) Yb $L_3$-edge for $Er_2O_3$, BYE and$Yb_2O_3$.

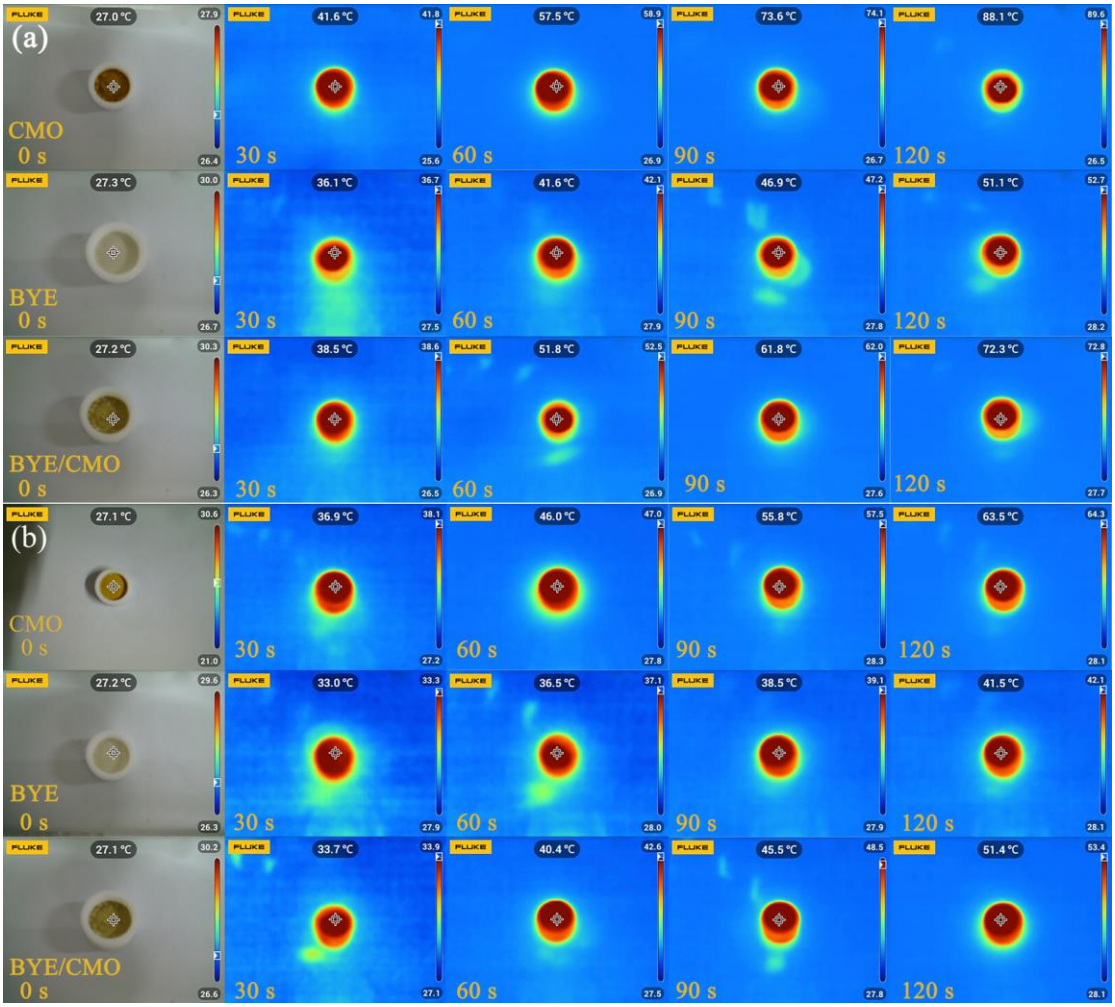


Fig. S4 The IR images of samples with different irradiation time under (a) Vis and (b) NIR light.

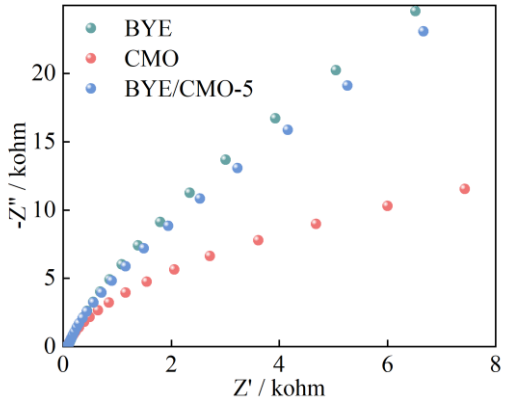


Fig. S5 Electrochemical impedance spectroscopy spectra of samples.

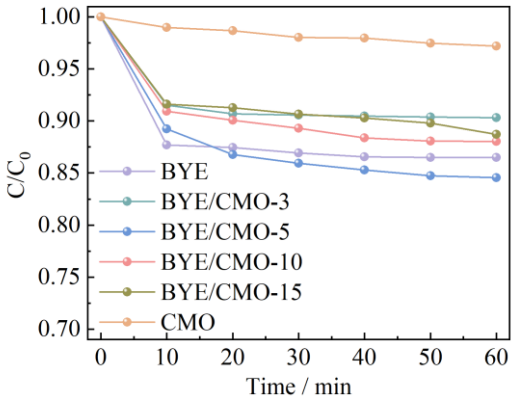


Fig. S6 Adsorption curves of MB over samples in dark.

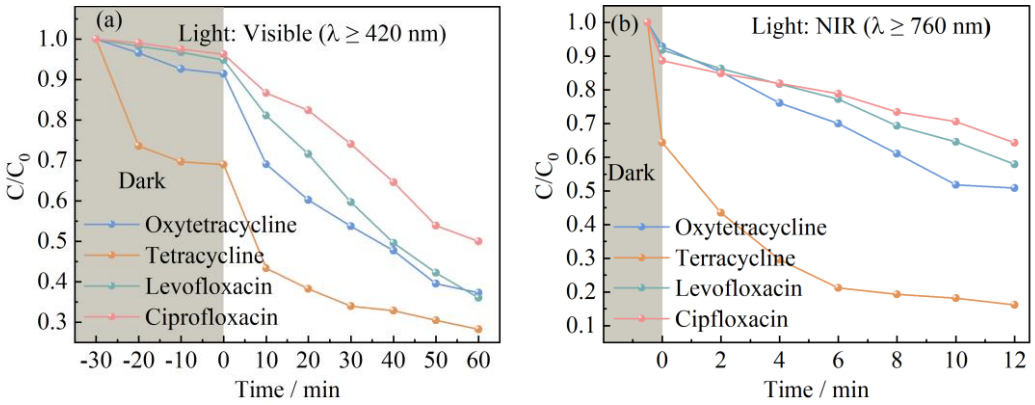


Fig. S7 Adsorption and photodegradation of typical antibiotic pollutants of BYE/CMO-5 under (a) Vis and (b) NIR light.

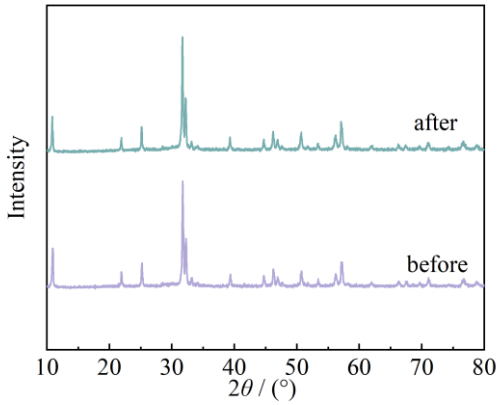


Fig. S8 XRD patterns of BYE/CMO-5 before and after photocatalysis.

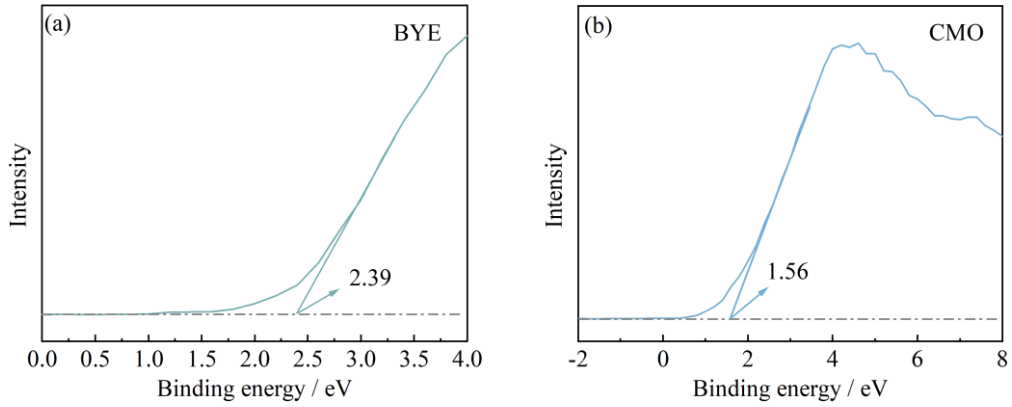


Fig. S9 Valence band XPS spectra of (a) BYE and (b) CMO.

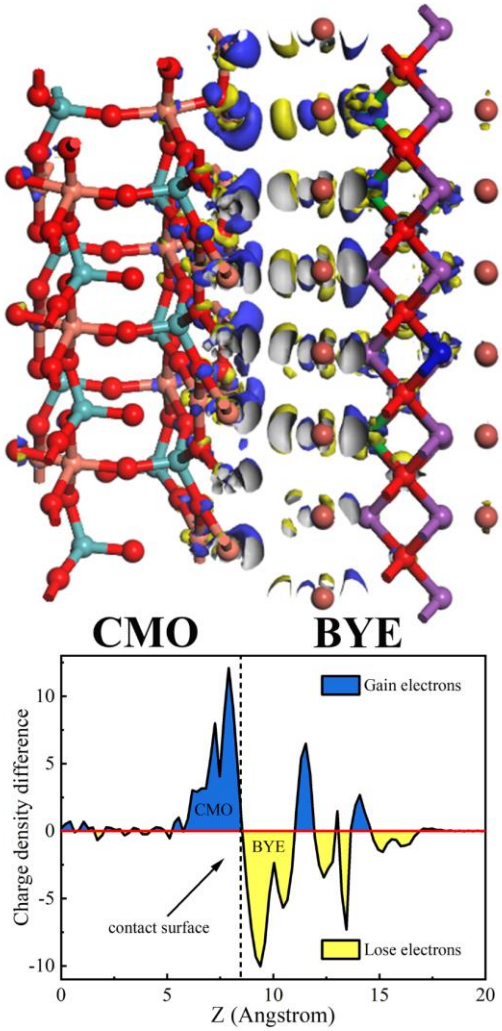


Fig. S10 Simulated charge distribution at the BYE/CMO interface at Fermi level equilibrium.

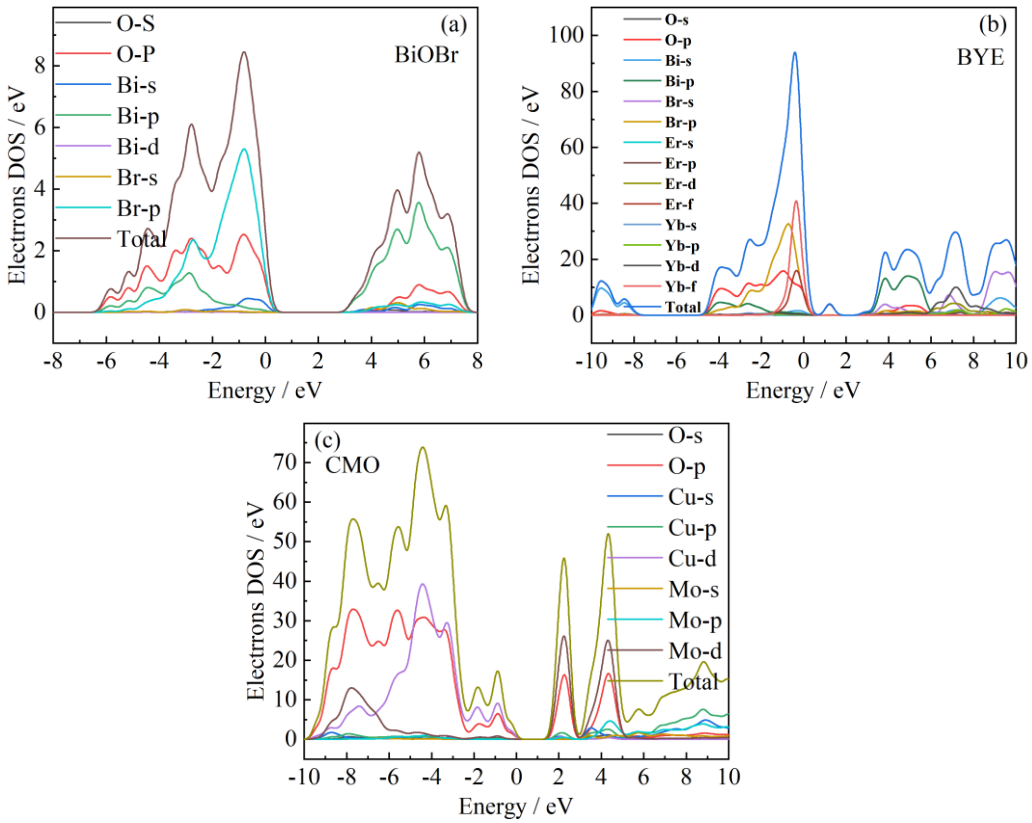


Fig. S11 The density of states plots of (a) BiOBr, (b) BYE and (c) CMO samples.

Table S1 BiOBr-based photocatalysts used for photodegradation of organic pollutants.

| **Kind of catalyst** | catalyst amount (mg/100 mL) | light source | Dye | Reaction time (min/h) | Degradation efficiency | Reference |
|---|---|---|---|---|---|---|
| BiOI:$Yb^{3+}$,$Er^{3+}$/$Bi_2O_4$ | 100 | Visible, 1000W halogen lamp NIR, 250 W infrared lamp | MB, 10 mg/L | 60 / 12 | 88% / 51% | This work |
| $Bi_2O_4$/BiOBr | 100 | Visible, 500W xenon lamp | MO, 10 mg/L | 60 | 99.3% | [1] |
| g-$C_3N_4$/BiOBr | 100 | Visible, 500W xenon lamp | RhB, 10 mg/L | 150 | 97.9% | [2] |
| AgBr/BiOBr/$NiFe_2O_4$ | 100 | Visible, 1000W halogen lamp | RhB, 20 mg/L | 90 | 100% | [3] |

| | | | | | | |
|---|---|---|---|---|---|---|
| $BiOBr/Bi_3O_4Br$ | 10 | Visible, 500W xenon lamp | RhB, 10mg/L | 90 | 97.1% | [4] |
| $BiOBr/BiVO_4:Yb^{3+},Er^{3+}$ | 20 | Visible, 300 W xenon lamp NIR, 980 nm-laser | MB, 10 mg/L | 120 /12 | 95.9% 69.7% | [5] |
| BiOBr@ZnFe-MOF | 15 | Visible, 300 W xenon lamp | MB, 5mg/L | 90 | 85.3% | [6] |
| $BiOBr/Zn_{0.5}Cd_{0.5}S$ | 100 | Visible, 300 W xenon lamp | MB, 20 mg/L | 240 | 99.52% | [7] |

**References**


1. Wang H Y, Liu Z S, Guo L T, Fan H L, Tao X Y. Novel $Bi_2O_4$/BiOBr heterojunction photocatalysts: In-situ preparation, photocatalytic activity and mechanism, Materials Science in Semiconductor Processing, 2018, 77: 8-15.
2. Zhou M, Huang W, Zhao Y, Jin Z, Hua X, Li K, Tang L. Cai Z, 2D g-$C_3N_4$/BiOBr heterojunctions with enhanced visible light photocatalytic activity. Journal of Nanoparticle Research, 2020, 22: 13.
3. Jiang X, Kong D Z, Luo B N, Wang M T, Zhang D F, Pu X P. Preparation of magnetically retrievable flower-like AgBr/BiOBr/$NiFe_2O_4$ direct Z-scheme heterojunction photocatalyst with enhanced visible-light photoactivity. Colloids and Surfaces A: Physicochemical and Engineering Aspects, 2022, 633: 127880.
4. Zhang F H, Xiao X Y, Xiao Y, In situ fabrication of type II 3D hierarchical flower-like BiOBr/$Bi_3O_4Br$ heterojunction with improved photocatalytic activity. Journal of Alloys and Compounds, 2022, 923: 166417.
5. Liu F, Zhang S C, Xu D, Sun F, Wang W L, Li X Y, Yu W S, Dong X T, Liu G X, Yu H. Columnar cactus-like 2D/1D BiOBr/$BiVO_4:Yb^{3+},Er^{3+}$ heterostructure photocatalyst with ultraviolet-visible-near infrared response for photocatalytic degrading dyes, endocrine disruptors and antibiotics. Journal of Alloys and Compounds, 2022 929: 167330.

6. Shi Y X, Wang L Y, Dong S H, Miao X, Zhang M X, Sun K, Zhang Y F, Cao Z Z, Sun J M. Wool-ball-like BiOBr@ZnFe-MOF composites for degradation organic pollutant under visible-light: Synthesis, performance, characterization and mechanism. Optical Materials, 2022, 131: 112580.
7. Qi S Y, Ma N L, Zhang R Y, Zhang Y M, Liu X T, Xu H Y. Preparation and photocatalytic properties of $Zn_{0.5}Cd_{0.5}S$/BiOBr heterojunction. Chemical Physics Letters, 2022, 791: 139381.